Electronic Journal of Differential Equations, Vol. 2013 (2013), No. 19, pp. 1–13.
ISSN: 1072-6691. URL: http://ejde.math.txstate.edu or http://ejde.math.unt.edu
ftp ejde.math.txstate.edu

SOLITARY WAVE COLLISIONS IN THE REGULARIZED LONG WAVE EQUATION

HENRIK KALISCH, MARIE HAI YEN NGUYEN, NGUYET THANH NGUYEN

Abstract. The regularized long-wave equation admits families of positive and negative solitary waves. Interactions of these waves are studied, and it is found that interactions of pairs of positive and pairs of negative solitary waves feature the same phase shift asymptotically as the wave velocities grow large as long as the same amplitude ratio is maintained. The collision of a positive with a negative wave leads to a host of phenomena, including resonance, annihilation and creation of secondary waves. A sharp criterion on the resonance for positive-negative interactions is found.

1. Introduction

This article is focused on the interaction of solitary-wave solutions to the regularized long-wave equation

$$u_t + u_x + (u^2)_x - u_{xxt} = 0, \tag{1.1}$$

which appears as a model equation for surface water waves. The equation is also known as the BBM or PBBM equation, as it first appeared in the work of Peregrine [36] and was studied in depth by Benjamin, Bona and Mahoney [6]. The equation was put forward as a model for small amplitude long waves on the surface of an inviscid incompressible fluid, and as such is an alternative to the well known Korteweg-de Vries (KdV) equation

$$u_t + u_x + (u^2)_x + u_{xxx} = 0. \tag{1.2}$$

Both (1.1) and (1.2) were derived as simplified models for unidirectional propagation of surface waves, but the regularized long wave equation has certain advantages, especially with regard to the numerical approximation of solutions containing components of shorter wavelength. Moreover, the linear phase speed of small periodic wave solutions of (1.1) resembles the actual phase speed of small amplitude surface waves as described by the Euler equations more closely than the KdV equation. In particular the phase velocity of small periodic solutions of (1.1) is always positive whereas the phase speed can turn negative in the KdV equation. For a more in-depth explanation of modeling aspects of these equations, one may consult [3, 6, 17, 41]. Despite the obvious advantages of (1.1), the KdV equation (1.2) has

2000 *Mathematics Subject Classification.* 35Q53, 35B34, 35C08.
Key words and phrases. Solitary waves; solitary-wave interaction; phase shift; resonance.

Submitted November 26, 2012. Published January 23, 2013.

become a generic model for the study of weakly nonlinear long waves in different types of modeling situations [1], thanks in part to the completely elastic interaction of its solitary waves [42].

In the context of (1.1) and (1.2), solitary-wave solutions may be defined as progressive waves which propagate without a change in their spatial profile, which have a single maximum or a single minimum, and which decay to zero for large absolute values of x. Elastic interaction may be described as follows. Suppose two solitary waves are arranged initially in such a way that one wave will pass the other wave (overtaking collision), or the two waves will meet head-on. In the KdV equation, which features only overtaking collision, both waves re-emerge unchanged, the only remnant of the interaction being a phase shift of both solitary waves. The discovery of the elastic interaction of two solitary waves was the first indication that the KdV equation may represent a completely-integrable, infinite-dimensional Hamiltonian dynamical system, and subsequently led to the discovery of an infinite number of time-invariant integrals [30], and the development of the inverse-scattering method which can be used to provide exact closed form solutions for a broad class of initial data [1, 19].

Regarding the equation (1.1), it was shown in [11] that even though the equation has closed form expressions for exact solitary-wave solutions, it does not feature elastic interaction of solitary waves. Indeed, as shown in Figure 3, interactions of solitary waves in the model (1.1) generally lead not only to a phase shift, but also to the creation of dispersive oscillations which remain after the interaction. This finding indicates that the equation (1.1) is not a completely integrable dynamical system, and in fact, non-integrability of (1.1) has been proved in [33]. Numerical studies of solitary-wave interactions have been used in a large number of cases to provide evidence against complete integrability. A sample of results are studies of the Benjamin and Benjamin-Ono equations [9, 24], a higher order compound KdV equation [26], a Boussinesq system for internal waves [31], and different types of equations for waves in solids [18, 40].

While equation (1.1) does not feature an infinite family of conserved quantities, it does have three independent invariant integrals, which are given by

$$I = \int_{-\infty}^{\infty} u\,dx, \qquad II = \int_{-\infty}^{\infty} \left(\tfrac{1}{2}u^2 + \tfrac{1}{2}u_x^2\right)\,dx, \quad III = \int_{-\infty}^{\infty} \left(\tfrac{1}{3}u^3 - \tfrac{1}{2}u_x^2\right)\,dx. \tag{1.3}$$

The solitary-wave solutions $u(x,t) = \psi_c(x-ct)$, of (1.1) are given in terms of the variable $\xi = x - ct$ in the form

$$\psi_c(\xi) = \frac{3}{2}(c-1)\,\mathrm{sech}^2\left(\tfrac{1}{2}\sqrt{\tfrac{c-1}{c}}\xi\right). \tag{1.4}$$

Now as opposed to the situation in the case of the KdV equation which features only positive solitary waves, the equation (1.1) admits both positive and negative solitary-wave solutions. Indeed, it is clear that the expression (1.4) actually defines two families of solitary waves. For the positive solutions, the velocity of the solitary wave is restricted by $c > 1$, and for the negative solutions, the velocity is restricted by $c < 0$. In both cases, the amplitude is given by $A = \frac{3}{2}|(c-1)|$. Wave profiles for a few positive and negative waves are shown in Figure 2.

The focus of the present article is two-fold. In Section 2, we compare the interactions of two positive and of two negative solitary waves. After extensive numerical

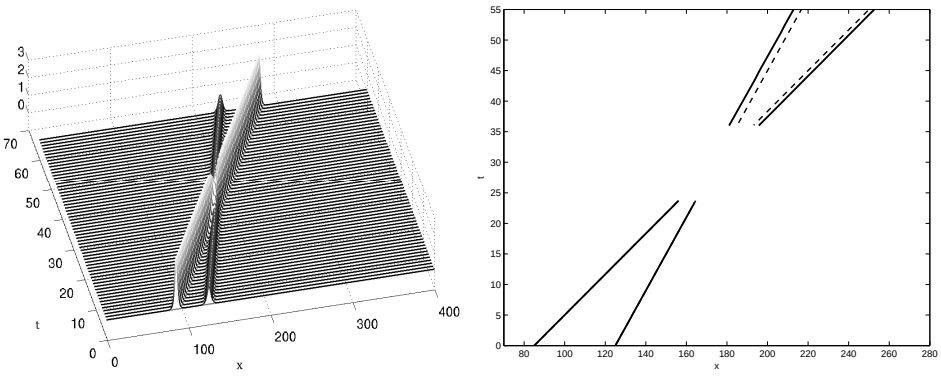

FIGURE 1. Interaction of two positive solitary waves in equation (1.1). The left panel shows the time evolution of the spatial profile. The scale is such that the dispersive tail due to the inelasticity cannot be seen. The right panel shows the positions of the maxima of the two waves as functions of t. The solid line shows the actual position of the maxima, while the dashed line indicates the position of the maxima in the case that no collision has taken place.

experimentation it appeared overtaking collisions are classified most effectively by keeping the amplitude ratio of the two interacting solitary waves constant. In clear terms, we study the interaction of a solitary wave of amplitude A with a smaller solitary wave of amplitude $\mathcal{R}A$, where $\mathcal{R}$ represents the ratio. If $\mathcal{R}$ is kept constant, then it will be shown in Section 2 that asymptotically as $A \to \infty$, the phase shifts of two interacting positive waves are equal to the phase shifts of two interacting negative waves.

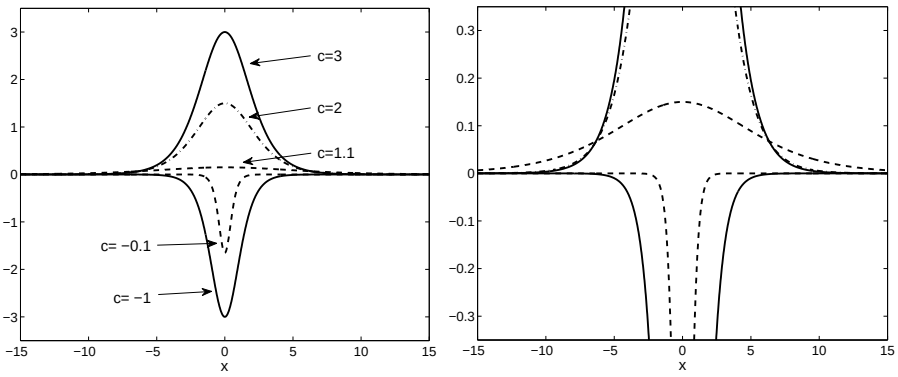

FIGURE 2. Positive and negative solitary wave profiles, for velocities $c = 1.1$, $c = 2$, $c = 3$, and $c = -0.1$, $c = -1$. The right panel shows a close-up of the waves which shows the different spatial decay of positive and negative solitary waves.

The second goal of this paper is the study of head-on collisions of solitary waves. Here, we investigate a regime in which the solitary waves are changed dramatically during the collision, as a considerable part of the available energy is fed into the nascent secondary solitary waves emerging after the interaction. This phenomenon was first discovered by Santarelli [38], and studied in depth by Courtenay Lewis and Tjon [16], who found that the occurrence of these secondary waves can be quantified in some sense using a resonance criterion based on the evaluation of the conserved integrals. However, the authors of [16] only found an asymptotic characterization of the resonance, and it is the purpose of the present work to show numerical evidence pointing to a sharp resonance criterion.

The numerical method to be used here is a Fourier-collocation method, where the nonlinear term is treated pseudo-spectrally. Even though this choice is standard, we recall it briefly in the appendix. The spectral method is coupled with an explicit four-stage Runge-Kutta scheme, and the resulting fully discrete code is highly stable and accurate. Indeed, it can be shown that the eigenvalues of the discrete linear operator fall squarely into the domain of A-stability of the Runge-Kutta method. Moreover, spectral convergence in the spatial discretization is observed, and indeed exponential convergence holds since the solitary waves used to test the convergence are analytic functions [7, 22, 32]. It should be mentioned that many other numerical methods for numerical approximation of solutions of (1.1) have been developed, and this is still an active area of research. Recent work featured both Galerkin methods [34], finite-difference methods [21], and collocation methods based on splines [37]. A pseudo-spectral method coupled with a leapfrog method for the time-discretization was proposed in [39], and methods for the study of solitary-wave evolution can be found in [4].

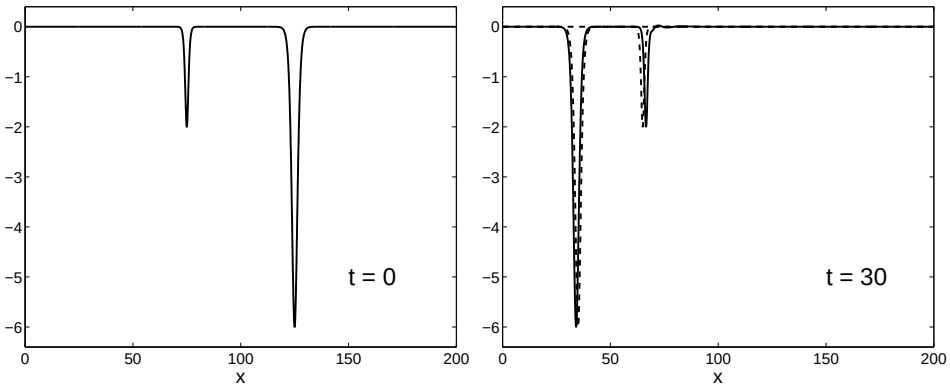

FIGURE 3. Interaction of two negative solitary waves. In the right panel, the phase shift and the production of dispersive oscillations behind the smaller solitary wave is clearly visible.

2. Overtaking collisions

The goal of this section is the comparison of overtaking collisions of two positive and of two negative solitary waves. For the comparison of overtaking collisions of a pair of positive and a pair of negative solitary waves, it appears most convenient to

require a constant ratio between the solitary-wave amplitudes, so that the parameter space may be defined by the single quantity $A = \frac{3}{2}|(c-1)|$ which represents the amplitude of the larger wave. Such an approach has actually been advocated in [13], where it was shown that the change in amplitude of the solitary waves after the interaction is dependent on the ratio of the amplitudes of the initial solitary waves. Amplitude changes after interactions have been investigated for positive solitary waves of (1.1) and for higher-order regularized equations [11, 16, 27], and it was noted in several previous works, that the change in amplitude is so slight that one might argue that the identity of the solitary waves is preserved, and it still makes sense to compute the phase shift of the waves.

Figure 4 shows the result of several runs with different amplitudes. If seen in relation to the direction of propagation, in both cases, the larger wave experiences a forward shift, while the smaller wave experiences a backward shift. In the left panel of Figure 4, the forward shift of the larger solitary wave after the interaction is plotted for both the positive and the negative wave. The amplitude ratio is fixed at $3:2$ in Figure 4, so that $\mathcal{R} = \frac{2}{3}$, both for the interaction of two positive waves and for the interaction of two negative waves. The data from the numerical runs for two positive waves are shown in the figures circles, and data for two negative waves are shown as dots. A rational curvefit is used for both the forward phase shift θ_L of the larger wave, and for the backwards shift θ_S of the smaller wave. The curve fit uses the simple model

$$|\theta_L| = \frac{P_1 A + P_2}{A + Q_1} \quad \text{and} \quad |\theta_S| = \frac{p_1 A + p_2}{A + q_1}.$$

The resulting horizontal asymptotes P_1 and p_1 are plotted as dashed lines. There is no visually discernible difference between the asymptotes, and the two asymptotic values P_1 and p_1 also lie within each other's confidence intervals for the curvefit.

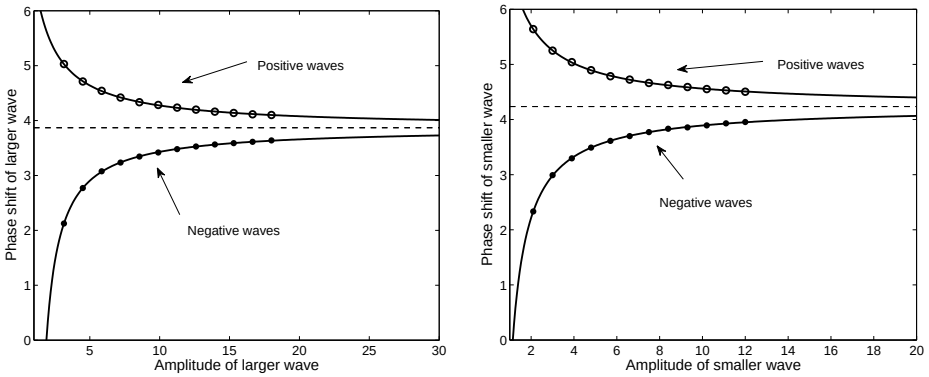

FIGURE 4. Overtaking collisions of a large and a small solitary wave with a constant amplitude ratio of $3:2$. The left panel shows the magnitude of the phase shift of the larger waves $|\theta_L|$, and the right panel shows the magnitude of the phase shift of the smaller waves $|\theta_S|$. The circles denote the interaction of two positive waves, and the dots denote the interaction of two negative waves. The solid curves represent a rational curve fit, and the dashed line is the horizontal asymptote of both curve fits.

The results of a similar study for a constant amplitude ratio $3:1$ are shown in Figure 5, and further test cases have been run for various other amplitude ratios. The results of these studies are all indicative of the basic relation that the phase shift in the small and large solitary wave are asymptotically equal after the interaction of a pair of positive and the interaction of a pair of negative solitary waves as long as the amplitude ratio $\mathcal{R}$ between the larger and the smaller wave is kept constant. Note that the magnitude of the phase shifts of two positive waves becomes very large for small amplitudes, while the phase shifts of two negative waves becomes rather smaller. If it is assumed that the phase shift is in some sense proportional to the interaction time, then the reason for this difference may be found in the different profiles of the positive and negative waves. Indeed, the positive waves become wider with decreasing amplitude, while the negative waves become narrower with decreasing amplitude (cf. Figure 2). Thus, in view of the relatively heavier tails, the interaction time is comparatively longer for two small positive solitary waves than it is for two small negative solitary waves, even though the velocities of the negative waves are smaller.

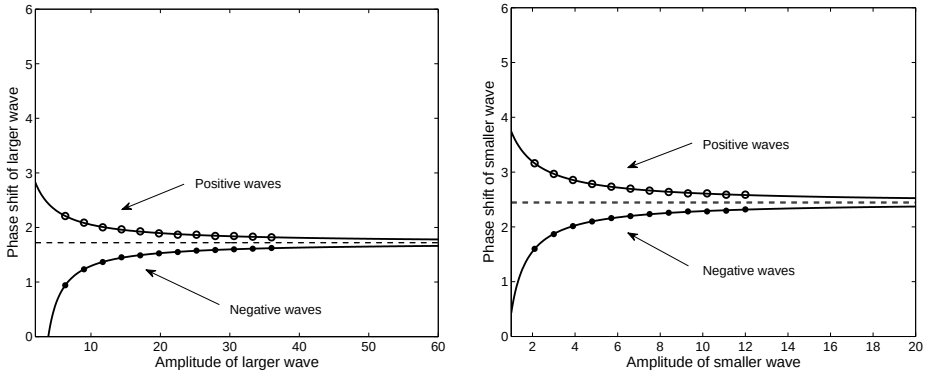

FIGURE 5. Overtaking collisions of a large and a small solitary wave with a constant amplitude ratio of $3:1$. The left panel shows the magnitude of the phase shift of the larger waves $|\theta_L|$, and the right panel shows the magnitude of the phase shift of the smaller waves $|\theta_S|$. The circles denote the interaction of two positive waves, and the dots denote the interaction of two negative waves. The solid curves represent a rational curve fit, and the dashed line is the horizontal asymptote of both curve fits.

3. Head on collisions

The inelasticity of the regularized long wave equation manifests itself somewhat differently in the case of two waves of opposite sign. While the interaction of two solitary waves of the same polarity produces only a dispersive tail, the collision of a positive and negative solitary wave can lead to the creation of secondary solitary waves in addition to a dispersive tail. It is also possible for two solitary waves of opposite polarity to be annihilated by the interaction.

The precise nature of a head-on collision depends on the two waves being close to resonance, and the outcome of the interaction near resonance may be characterized

as follows. If both solitary waves are of small amplitude, then annihilation takes place. In other words, the only remaining disturbance after the interaction is a dispersive tail (see Fig. 5 in [16]). For larger amplitudes, the waves re-emerge out of the dispersive tail, and for even larger amplitudes, secondary solitary waves appear after the interaction. A typical case of a resonant interaction of two large amplitude wave of opposite polarity is shown in Figure 6.

In the following, a numerical study of head-on collisions is presented, and a sharp resonance criterion for the interaction of a positive and a negative solitary wave is exhibited. This result is an improvement upon the work of Courtenay Lewis and Tjon [16], who investigated the resonance which was originally discovered by Santarelli [38]. Denoting the positive solitary wave by ψ_{c_p}, and the negative solitary wave by ψ_{c_n}, the resonance criterion was given by Courtenay Lewis and Tjon [16] in terms of $I_n = \int \psi_{c_n}$ and $I_p = \int \psi_{c_p}$ by $I_p + I_n = 0$. Indeed, using

$$r = \frac{I_p + I_n}{I_p - I_n}$$

to parameterize the trial space, they found the resonance near but not on the line $r = 0$. Moreover, it was found that as the total area $I_p - I_n$ increases, the resonance moved closer to the line $I_p + I_n = 0$, which can be written in terms of the phase velocities as

$$c_p + c_n = 1. \tag{3.1}$$

While the use of I to parameterize the trial space may appear natural from the viewpoint of completely integrable differential equations, viewing the solution set as parameterized by the wave speed c is more useful for pinpointing the exact resonance condition. As will be clear from the numerical experiments presented here, the resonance can be characterized explicitly by the condition

$$c_p + c_n = 0.85. \tag{3.2}$$

In order to facilitate comparison with the work in [16], we choose the same method to quantify the resonance by way of the invariant integral II. In fact, as noted in [16], one may use any one of the three conserved integrals I, II III, or a linear combination of these, but the advantage of II is that it is automatically positive throughout a computation. Owing to the fast decay of the exact solitary-wave solutions, one may define these integrals for individual components of initial data. So if initial data are taken to be $u_0 = \psi_{c_p}(x) + \psi_{c_n}(x-\tau)$, then one may define $II_p = II(\psi_{c_p})$ and $II_n = II(\psi_{c_n})$. The same may be done after an interaction if the waves have separated from each other, and from any dispersive residue. This leads to II_p^f and II_n^f, where the superscripts indicate that the integrals are computed at the final time after the interaction. Now to quantify the resonance, one may use the quantity

$$\kappa = 1 - \frac{II_p^f + II_n^f}{II_p + II_n}.$$

Note that κ is always between 0 and 1, and $\kappa = 0$ signifies the case where both solitary waves re-emerge unchanged from the interaction. For the equation (1.1), κ is never exactly zero, because of the inelasticity. On the other hand, the value $\kappa = 1$ indicates that the original solitary waves have completely disappeared.

Figure 7 shows the result of a number of numerical runs for positive-negative solitary-wave interactions. In the left panel, the resonance parameter κ is graphed against the sum of the velocities $c_p + c_n$. It is plain from the figure that the largest

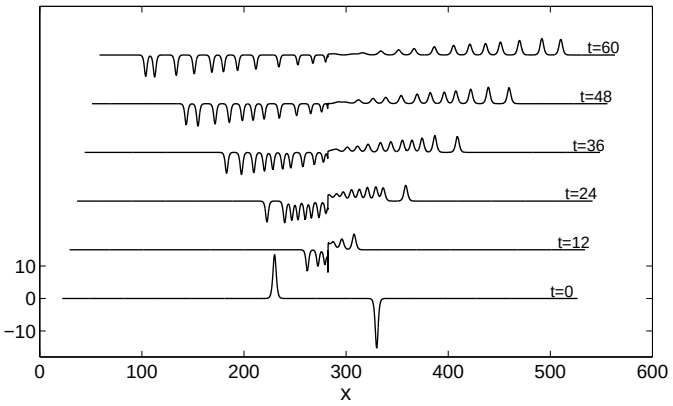

FIGURE 6. Interaction of a positive and a negative solitary wave at resonance. The wave speed of the positive solitary wave is $c = 10$. The wave speed of the negative solitary wave is $c = -9.15$. The figure shows snapshots of the solutions at different times, as indicated at the right end of the respective curve. A violent, nearly singular interaction can be seen, and the formation of secondary solitary waves is observed as the main waves pull from the interaction region.

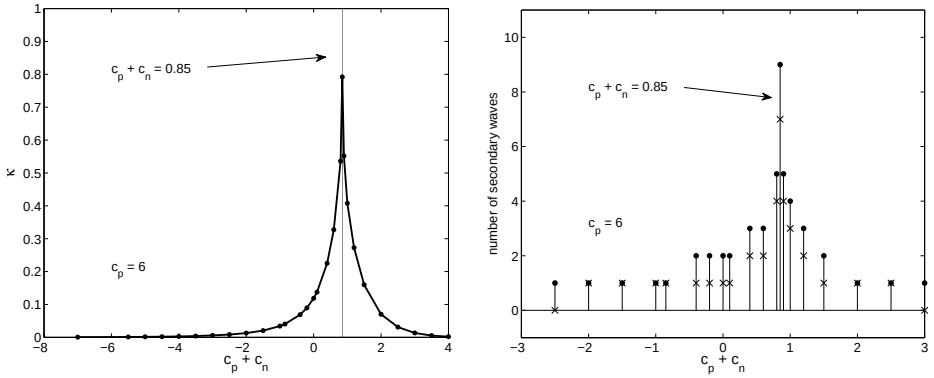

FIGURE 7. The left panel displays the inelasticity κ of the head-on collision of a positive and a negative solitary wave as a function of c_p+c_n. The positive solitary wave is kept constant at the speed $c_p = 6$, and the velocity of the negative solitary wave is varied. The largest value of κ appears precisely at $c_p + c_n = 0.85$. The right panel shows data from the same experiments, and records the number of secondary positive and negative solitary waves created after the collision. The number of positive secondary waves is graphed with dots, and the number of negative waves is graphed with an $\times$.

value of κ occurs precisely on the line $c_p + c_n = 0.85$. The right panel of Figure 7 indicates the number of secondary solitary waves created by the collision of the original waves, and it is again clear that the maximal number of secondary waves is achieved exactly on the line $c_p + c_n = 0.85$. Figure 8 displays the results of

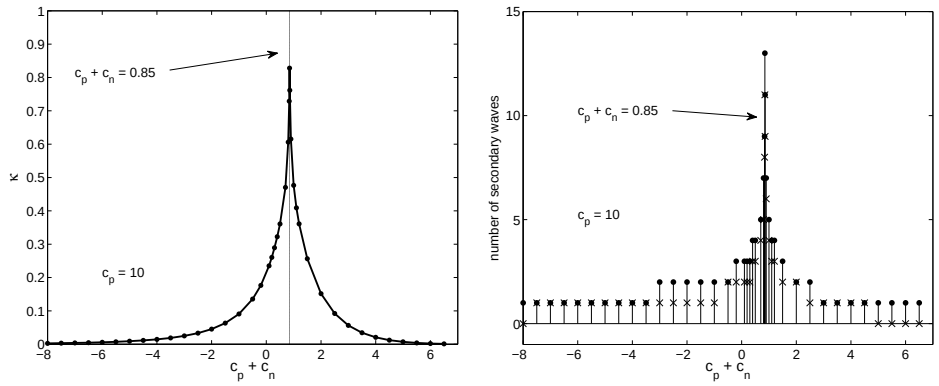

FIGURE 8. The left panel displays the inelasticity κ of the head-on collision of a positive and a negative solitary wave as a function of c_p+c_n. The positive solitary wave is kept constant at the speed $c_p = 10$, and the velocity of the negative solitary wave is varied. The largest value of κ appears precisely at $c_p + c_n = 0.85$. The right panel shows data from the same experiments, and records the number of secondary positive and negative solitary waves created after the collision. The number of positive secondary waves is graphed with dots, and the number of negative waves is graphed with an $\times$.

similar runs but now with a positive wave of fixed phase speed $c = 10$. Note that the number of secondary waves is higher in these trials, and it appears that by choosing initial solitary waves of large enough speed, one may create any number of secondary waves.

4. Conclusions

In this paper, two aspects of solitary-wave interactions were investigated. First, the overtaking collision of a pair of positive and a pair of negative solitary waves was compared, and it was shown numerically that the phase shift of the waves is asymptotically equal if the amplitude ratio of the waves is held constant. The approach is in line with previous work [13, 27] which suggested the amplitude ratio as a convenient measure for properties of solitary-wave interactions.

Secondly, the head-on collision of a pair of solitary waves of opposite polarity was studied. It was shown that the resonance parameter κ is a convenient measure for the behavior of the solution, and that resonance occurs precisely on the line $c_p + c_n = 0.85$. This resonance condition is an improvement upon previously available results. At and near resonance, creation of secondary solitary waves is observed. Annihilation is observed when the amplitudes of the solitary waves are sufficiently small.

While the equation (1.1) is known to be a reasonable model for long waves of small amplitude and negligible transverse variation, it is also apparent that most of the waves shown in this paper have large amplitude, so that they do not lie within the regime of physical applicability of equation (1.1) as a long wave model for surface water waves. However, since (1.1) is one of the key models for water waves,

it is also important to have a solid understanding of the dynamics of solutions from a mathematical point of view.

In the case of the KdV equation (1.2), the inverse-scattering theory [1] provides a convenient framework of the mathematical study of the equations. In the case of (1.1), these methods are not available, and therefore the analysis of mathematical properties is more difficult. Nevertheless, a number of rigorous results exists, such as proofs of well posedness [6, 14], and studies investigating the relation between the periodic and pure Cauchy problem [15, 35]. Some recent work focuses on establishing precise estimates on the change in amplitude and the phase shift in the overtaking collision of two positive solitary waves [28, 29], but it is unclear whether these techniques will also apply to solitary-wave interactions featuring one or two negative solitary waves.

The dynamic stability of positive solitary was established some time ago [5, 8, 20], and has also been studied numerically [10]. However, small negative waves may be unstable, as explained in [23], and proved in [25, 32]. The instability of small negative solitary waves may be explained by the inability of coherent structures to withstand the dispersion of the linear part of the equation [2]. This phenomenon may also be invoked to explain the annihilation of a positive and a negative solitary wave in a head-on collision. One may think of the interaction as conserving the total energy $II(u)$, and if the two solitary waves are near resonance, then the energy is fed into secondary waves. However, due to the instability of small negative solitary waves, the secondary negative wave disperses immediately. This also explains why the number of negative secondary waves is generally smaller than the number of positive secondary waves.

5. Appendix: The numerical technique

The spectral projection of the initial-value problem associated to the evolution equation (1.1) is briefly recalled. In order to approximate the problem on the real line, a large interval $[0, L]$ is chosen. The problem is then translated to the interval $[0, 2\pi]$ by the scaling $u(ax, t) = v(x, t)$, where $a = \frac{L}{2\pi}$. The evolution equation satisfied by v is then

$$a^2 v_t(x,t) + a v_x(x,t) + a(v^2)_x(x,t) - v_{xxt}(x,t) = 0, \quad x \in [0, 2\pi],\ t > 0,$$

and the initial-value problem is obtained by setting periodic boundary conditions $v(0, t) = v(2\pi, t), t \geq 0$, and initial data $v(x, 0) = u_0(ax), x \in [0, 2\pi]$. This approach is standard, and may be found in any treatment of spectral methods. A discussion regarding different aspects of the approximation of the problem on the real line by a periodic problem may be found in [15] and [35]. Discretizing using a Fourier collocation method yields

$$\begin{gathered}\frac{\partial}{\partial t}\hat{v}_N(k,t) = -\frac{aik}{a^2+k^2}\Big\{\hat{v}_N(k,t) + \mathcal{F}\Big(\big[\mathcal{F}^{-1}(\hat{v}_N)\big]^2\Big)\Big\}, \\ k = -\frac{N}{2}+1, \dots, \frac{N}{2},\ t > 0,\end{gathered} \tag{5.1}$$

where $\mathcal{F}$ is the discrete Fourier transform defined for an arbitrary continuous function w by $\mathcal{F}w(k) = \frac{1}{N}\sum_{j=0}^{N-1} e^{-ikx_j} w(x_j)$. The symbol $\mathcal{F}^{-1}$ denotes the discrete inverse Fourier transform, given by $\mathcal{F}^{-1}(\hat{w}, x_j) = \sum_{k=-\frac{N}{2}+1}^{\frac{N}{2}} e^{ikx_j}\hat{w}(k,t)$, evaluated at the collocation points $x_j = \frac{2\pi j}{N}$, for $j = 1, \dots, N$. The system (5.1) is a system

of N ordinary differential equations for the discrete Fourier coefficients $\hat{v}_N(k,t)$, for $k = -\frac{N}{2}+1, \dots, \frac{N}{2}$. As is customary, the coefficient $\hat{v}_N(\frac{N}{2},t)$ is set to zero, but carried along for the discrete Fourier transform. We integrate the system by using a four-stage explicit Runge-Kutta scheme with a uniform time step h. To test the convergence of the algorithm and the numerical implementation, the normalized discrete L^2-norm is used. This norm is defined by

$$\|v(\cdot,t)\|_{N,2}^2 = \frac{1}{N}\sum_{i=1}^{N} |v(x_i,t)|^2.$$

The relative L^2-error is then defined to be

$$\text{Error} = \frac{\|v - v_N\|_{N,2}}{\|v\|_{N,2}},$$

where $v(x_i,t)$ is the exact solution, and $v_N(x_i,t)$ is the numerical approximation at a specific time t. In order to test the implementation of the algorithm, the evolution of a solitary-wave solution is computed numerically, and then compared to the exact solutions obtained by translating the wave by an appropriate distance. Table 1 displays the outcome of several runs with varying number of modes N and time step h. It is clear that both the required 4-th order convergence in terms of the time step h and the spectral convergence in terms of the number of spatial grid points N is achieved.

Temporal discretization			Spatial discretization		
h	Error	ratio	N	Error	ratio
0.1000	7.8226e-05		1024	4.921e-01	
0.0500	4.4138e-06	17.723	2048	2.378e-01	2.07
0.0250	2.6056e-07	16.940	4096	2.125e-02	11.19
0.0125	1.5801e-08	16.490	8192	1.968e-04	107.69
0.0063	9.7229e-10	16.251	16384	2.431e-08	8097.02
0.0031	6.0236e-11	16.142	32768	1.335e-09	1.82
0.0016	3.7116e-12	16.230			
0.0008	2.1690e-13	17.112			

TABLE 1. Discretization errors arising on a domain $[0, 200]$, at the final time $T = 8$. The first three columns show errors achieved with a fixed number of grid points $N = 4096$. The last three columns show errors achieved with a fixed time step of $h = 0.001$.

Acknowledgements. This research was supported in part by the Research Council of Norway through grant no. NFR 213474/F20.

REFERENCES

[1] M. Ablowitz, H. Segur; *Solitons and the Inverse Scattering Transform*, SIAM Studies in Applied Mathematics **4** (SIAM, Philadelphia, 1981).

[2] J. P. Albert; *Dispersion of low-energy waves for the generalized Benjamin-Bona-Mahoney Equation.* J. Differential Equations **63** (1986), 117–134.

[3] J. P. Albert, J. L. Bona; *Comparisons between model equations for long waves.* J. Nonlinear Sci. **1** (1991), 345–374.

[4] J. Álvarez, A. Durán; *On the preservation of invariants in the simulation of solitary waves in some nonlinear dispersive equations*. Commun. Nonlinear Sci. Numer. Simul. **17** (2012), 637–649.
[5] T. B. Benjamin; *The stability of solitary waves*. Proc. R. Soc. London A **328** (1972), 153–183.
[6] T. B. Benjamin, J. B. Bona, J. J. Mahony; *Model equations for long waves in nonlinear dispersive systems*. Philos. Trans. R. Soc. London A **272** (1972), 47–78.
[7] M. Bjørkavåg, H. Kalisch; *Exponential convergence of a spectral projection of the KdV equation*. Phys. Lett. A **365** (2007), 278–283.
[8] J. L. Bona; *On the stability theory of solitary waves*. Proc. R. Soc. Lond. A **344** (1975), 363–374.
[9] J. L. Bona, H. Kalisch; *Singularity formation in the generalized Benjamin-Ono equation*. Discrete Contin. Dyn. Syst. **11** (2004), 779–785.
[10] J. L. Bona, W. R. McKinney, J. M. Restrepo; *Stable and unstable solitary-wave solutions of the generalized regularized long-wave equation*. J. Nonlinear Sci. **10** (2000), 603–638.
[11] J. L. Bona, W. G. Pritchard, L.R. Scott; *Solitary-wave interaction*. Phys. Fluids **23** (1980), 438-441.
[12] J. L. Bona, P. E. Souganidis, W. A. Strauss; *Stability and instability of solitary waves of Korteweg-de Vries type*. Proc. R. Soc. Lond. A **411** (1987), 395–412.
[13] J. G. B. Byatt-Smith; *On the change of amplitude of interacting solitary waves*. J. Fluid Mech. **182** (1987), 485–497.
[14] H. Chen; *Periodic initial-value problem for BBM-equation*. Comput. Math. Appl. **48** (2004), 1305–1318.
[15] H. Chen; *Long-period limit of nonlinear dispersive waves: the BBM-equation*. Differential Integral Equations **19** (2006), 463–480.
[16] J. Courtenay Lewis, J. A. Tjon; *Resonant production of solitons in the RLW equation*. Phys. Lett. A **73** (1979), 275–279.
[17] M. Ehrnström, H. Kalisch; *Traveling waves for the Whitham equation*. Differential Integral Equations **22** (2009), 1193–1210.
[18] J. Engelbrecht, A. Salupere, K. Tamm; *Waves in microstructured solids and the Boussinesq paradigm*. Wave Motion **48** (2011), 717–726.
[19] C. S. Gardner, J. M. Green, M. D. Kruskal, R. M. Miura; *A method for solving the Korteweg-de Vries equation*. Phys. Rev. Lett. **19** (1967), 1095–1097.
[20] M. Grillakis, J. Shatah, W.A. Strauss, *Stability theory of solitary waves in the presence of symmetry*. J. Funct. Anal. **74** (1987), 160–197.
[21] L. Iskandar, M. Sh. E.-D. Mohamedein; *Solitary waves interaction for the BBM equation*. Comput. Methods Appl. Mech. Engrg. **96** (1992), 361–372.
[22] H. Kalisch; *Rapid convergence of a Galerkin projection of the KdV equation*. C. R. Math. Acad. Sci. Paris, **341** (2005), 457–460.
[23] H. Kalisch; *Solitary Waves of Depression*. J. Comput. Anal. Appl. **8** (2006), 5–24.
[24] H. Kalisch, J. L. Bona; *Models for internal waves in deep water*. Discrete Contin. Dyn. Syst. **6** (2000), 1–19.
[25] H. Kalisch, N.T. Nguyen; *Stability of negative solitary waves*. Electron. J. Differential Equations **2009** no. 158, 1-20.
[26] O. E. Kurkina, A. A. Kurkin, E. A. Rouvinskaya, E. N. Pelinovsky, T. Soomere; *Dynamics of solitons in non-integrable version of the modified Korteweg-de Vries equation*. JETP Letters **95** (2012), 91–95.
[27] T. R. Marchant; *Solitary wave interaction for the extended BBM equation*. Proc. R. Soc. Lond. A **456** (2000), 433–453.
[28] Y. Martel, F. Merle; Inelastic interaction of nearly equal solitons for the BBM equation. Discrete Contin. Dyn. Syst. **27** (2010), 487–532.
[29] Y. Martel, F. Merle and T. Mizumachi, *Description of the inelastic collision of two solitary waves for the BBM equation*. Arch. Ration. Mech. Anal. **196** (2010), 517–574.
[30] R. M. Miura, C. S. Gardner, M. D. Kruskal; *Korteweg-de Vries equation and generalizations. II. Existence of conservation laws and constants of motion*. J. Math. Phys. **9** (1968), 1204–1209.
[31] H. Y. Nguyen, F. Dias; *A Boussinesq system for two-way propagation of interfacial waves*. Phys. D **237** (2008), 2365–2389.

[32] N. T. Nguyen, H. Kalisch; *Orbital stability of negative solitary waves*. Math. Comput. Simulation **80** (2009), 139–150.
[33] P. J. Olver; *Euler operators and conservation laws of the BBM equation*. Math. Proc. Cambridge Philos. Soc. **85** (1979), 143–160.
[34] K. Omrani; *The convergence of fully discrete Galerkin approximations for the Benjamin-Bona-Mahony (BBM) equation*. Appl. Math. Comp. **180** (2006), 614–621.
[35] J. Pasciak; *Spectral methods for a nonlinear initial-value problem involving pseudodifferential operators*, SIAM J. Numer. Anal. **19** (1982), 142–154.
[36] P. G. Peregrine; *Calculations of the development of an undular bore*. J. Fluid Mech. **25** (1966), 321–330.
[37] K. R. Raslan and M. S. Hassan; *Solitary waves for the MRLW equation*. Appl. Math. Lett. **22** (2009), 984–989.
[38] A. R. Santarelli; *Numerical analysis of the regularized long-wave equation: anelastic collision of solitary waves*. Nuovo Cimento Soc. Ital. Fis. B **46** (1978), 179–188.
[39] D. M. Sloan; *Fourier pseudospectral solution of the regularised long wave equation*. J. Comput. Appl. Math. **36** (1991), 159–179.
[40] K. Tamm, A. Salupere; *On the propagation of 1D solitary waves in Mindlin-type microstructured solid*. Math. Comput. Simulation **82** (2012), 1308–1320.
[41] G. B. Whitham; *Linear and Nonlinear Waves* (Wiley, New York, 1974).
[42] N. J. Zabusky, M. D. Kruskal; *Interaction of solutions in a collisionless plasma and the recurrence of initial states*. Phys. Rev. Lett. **15** (1965) 240–243.

Henrik Kalisch
Department of Mathematics, University of Bergen, Postbox 7800, 5020 Bergen, Norway
E-mail address: henrik.kalisch@math.uib.no

Marie Hai Yen Nguyen
Laboratoire de météorologie dynamique, Université Paris 6, 75252 Paris Cedex 05, France
E-mail address: mathsyen@yahoo.com

Nguyet Thanh Nguyen
Department of Mathematics, University of Bergen, Postbox 7800, 5020 Bergen, Norway
E-mail address: nguyen.nguyet13@yahoo.com